Int J Adv Manuf Technol (2007) 33:110–118
DOI 10.1007/s00170-007-0953-8

ORIGINAL ARTICLE

Comparison of optical and stylus methods for measurement of surface texture

T. V. Vorburger · H.-G. Rhee · T. B. Renegar · J.-F. Song · A. Zheng

Received: 24 January 2006 / Accepted: 17 January 2007 / Published online: 7 February 2007

Abstract Optical methods are increasingly used for measurement of surface texture, particularly for areal measurements where the optical methods are generally faster. A new Working Group under Technical Committee (TC) 213 in the International Organization for Standardization is addressing standardization issues for areal surface texture measurement and characterization and has formed a project team to address issues posed by the optical methods. In this paper, we review the different methods of measuring surface texture and describe a classification scheme for them. We highlight optical methods and describe some of their characteristics as well as compare surface-profiling results obtained from three optical methods with those obtained from stylus profiler instruments. For moderately rough surfaces ($Ra \approx 500$ nm), roughness measurements obtained with white light interferometric (WLI) microscopy, confocal microscopy, and the stylus method seem to provide close agreement on the same roughness samples. For surface roughness measurements in the 50 to 300 nm range of *Ra*, discrepancies between WLI and the stylus method are observed. In some cases the discrepancy is as large as about 75% of the value obtained with the stylus method. By contrast, the results for phase shifting interferometry over its expected range of application are in moderately good agreement with those of the stylus method.

Keywords Surface · Metrology · Stylus · Interferometric · Microscopy · Confocal · White light · Optical

1 Introduction

Surface texture affects the function of many types of industrial products ranging from roadways and mechanical parts to semiconductors and optics. Moreover, a wide range of methods have been developed for measuring surface texture [1] to the extent that it is difficult to sort out their various strengths and limitations to ascertain which methods are suitable for which measurement applications.

In 2002, the International Organization for Standardization (ISO) Technical Committee (TC) 213, dealing with Dimensional and Geometrical Product Specifications and Verification, formed a working group (WG) 16 to address standardization of areal (3D) surface texture measurement methods as well as review existing standards on traditional profiling (2D) methods. Working Group 16 is developing a number of draft standards encompassing definitions of terms and parameters, calibration methods, file formats, and characteristics of instruments. Under this working group, a project team is developing standards for optical methods of areal surface texture measurement. In one of these draft standards, surface texture measurement methods are classified into three types: line profiling, areal topography, and area integrating, as shown in Fig. 1 [2, 3].

A line-profiling method uses a high-resolution probe to sense the peaks and valleys of the surface topography and produce a quantitative profile $Z(X)$ of the surface topogra-

T. V. Vorburger (✉) · H.-G. Rhee · T. B. Renegar · J.-F. Song · A. Zheng
National Institute of Standards and Technology,
Gaithersburg, MD 20899, USA
e-mail: tvtv@nist.gov

Present address:
H.-G. Rhee
Korea Research Institute of Standards and Science,
Taejon 305-600, South Korea

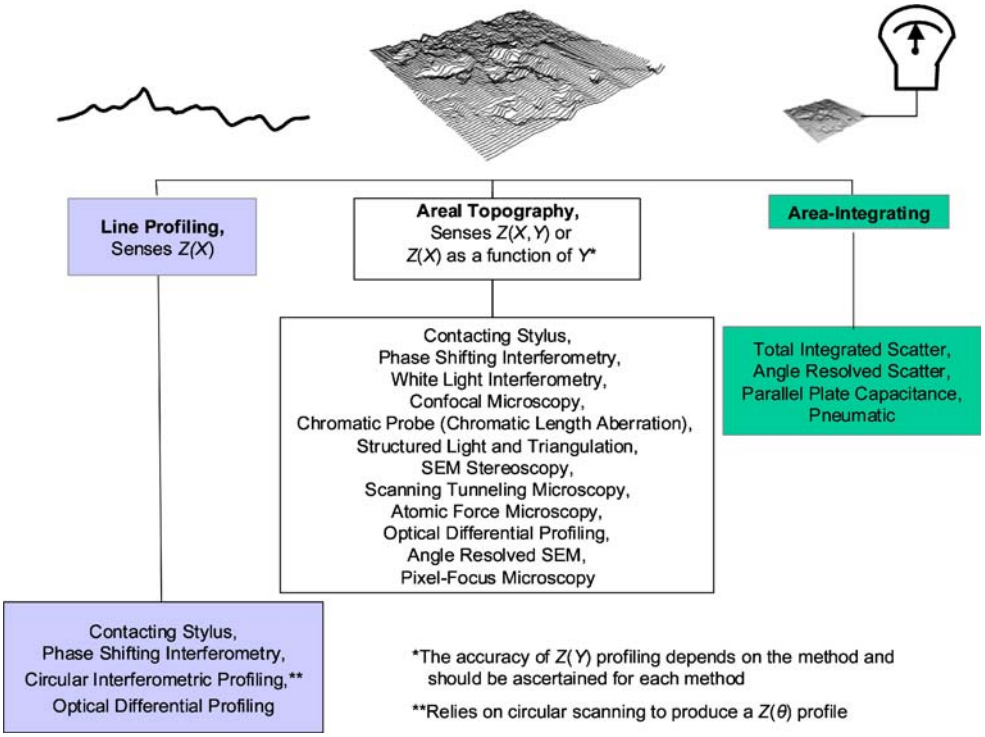

Fig. 1 Classification of surface texture measurement methods with examples shown for each class [2, 3]. Note that the term "areal topography" itself is under review by the ISO working group developing this chart and may be revised

phy. Areal topography methods extend the line-profiling method into three dimensions, usually by rastering a series of parallel profiles or by some quantitative topographic imaging process. It is important to note that some types of areal profiling methods can sense *Z*-height as a function of both the *X*- and *Y*-coordinates, whereas others may display topographic images with a series of parallel *Z*(*X*) profiles whose relative heights along the *Y*-direction may be somewhat arbitrary.

Area-integrating methods probe an area of the surface all at once to produce a quantity that represents some statistical average of the surface peaks and valleys.

Examples of these types of methods are listed in Fig. 1. In this paper we will focus on line profiling and areal topography methods and in particular on the widely used stylus-profiler method, phase-shifting interferometry (PSI), white light interferometry (WLI) and confocal microscopy. Important qualities of these instruments include the vertical resolution, the lateral or spatial resolution, and any factors that affect their ability to sense surface topography accurately.

1.1 Contacting methods

The stylus profiler senses the surface height through mechanical contact where a stylus traverses the peaks and valleys of the surface with a small contacting force. The vertical motion of the stylus is converted to an electrical signal by a transducer, which represents the surface profile *Z*(*X*) or topography image *Z*(*X,Y*). The vertical resolution can be as small as approximately 0.05 nm [4]. The lateral resolution is limited by the size of the stylus tip, which can be as small as about 100 nm [5]. The stylus position depends on little else than repulsive mechanical contact with the surface. Therefore, the stylus method is directly sensitive to surface height with little interference. One disadvantage of stylus instruments, however, is that the stylus may damage the surface, depending on the hardness of the surface relative to the stylus normal force and tip size.

Atomic force microscopes (AFMs) [6] are similar to stylus instruments insofar as they usually work through repulsive mechanical contact. But these sensors have greater sensitivity and incorporate force feedback and null sensing and often include vibrating tips with AC feedback. AFMs are capable of sub-tenth nanometer vertical resolution. However, because topography images are developed by a sequential series of profiles and AFMs are generally used to measure extremely smooth surfaces with small Z-values, drift is a limiting source of uncertainty for developing Z(*Y*) information with AFMs.

Both AFMs and stylus instruments have a lateral resolution that is limited by the interaction of the probe tip in contact with the peaks and valleys of the surface [7, 8]. Because their tip sizes and contact forces are smaller than those of stylus instruments, AFMs are capable of near-atomic spatial resolution [9] when used to measure smooth surfaces with small slopes. However, for surfaces with slopes of a few degrees or more, AFMs tend to lose this advantage because many points on the tip interact by turns with the surface. In such cases, the tip-surface contact for both stylus instruments and AFMs can produce significant dilation [7],

resulting in the broadening of peaks and narrowing of valleys in the measured profiles or topographies.

1.2 Optical techniques

A number of optical methods have been developed for line profiling and areal topography. Nearly all of them can provide spatial resolution approaching the diffraction limit of optical microscopy, which is about 500 nm for visible light illumination. Optical methods have been reviewed recently by Hocken et al. [10].

Optical methods have the advantage that they are non-contacting and hence, non-destructive. Optical methods based on imaging and microscopy also have a higher speed than contacting techniques, which rely on mechanical scanning of a contacting probe. However, optical methods are sensitive to a number of surface qualities besides the surface height. These include optical constants, surface slopes, fine surface features that cause diffraction, and deep valleys in which multiple scattering may occur. In addition, scattering from surfaces within the optical system produces stray light in the system that can affect the accuracy of an optical profiling method.

More sensitive methods, such as phase shifting interferometric (PSI) microscopy [11, 12], have vertical resolution on the order of 0.1 nm. By contrast, white light interferometric (WLI) [13, 14] microscopy and confocal microscopy [15] have a large vertical range, which is limited mainly by the range of the motion stage used to drive the vertical scan of the instrument and is often on the order of a millimeter.

WLI microscopy [13, 14] uses a broadband light source. The optical system focuses the light through a microscope objective onto a surface. An interferometer just below or above the objective splits the light into two parts, one directed to the surface and the other directed to a smooth reference mirror. When the reflected beams are recombined, interference fringes are produced around the equal path condition for the two beams. This equal path condition can be detected for each local area of the surface corresponding to each pixel of the camera detector. Scanning the surface vertically with respect to the microscope and detecting the optimum equal path condition at every pixel in the camera results in a topographic image.

Confocal microscopy [15] describes a class of methods that use apertures to sense the height of a surface point with respect to the best focus position in the microscope. Light reflected from a surface point passes through the aperture if the aperture is located at the best focus position with respect to the surface and the objective. One can determine the height of a point on the surface by scanning the surface vertically with respect to the aperture and objective and measuring the signal strength through the aperture as a function of vertical scan position. In alternative designs, other components in the optical path may be scanned. An areal topography image is then produced either by a multi-aperture (Nipkow disk) approach or by scanning the aperture laterally with respect to the surface.

WLI and confocal microscopy seem particularly versatile. PSI is limited to smooth surfaces, whereas the vertical dynamic range of WLI and confocal microscopy extends from the nanometer level (noise) to a large range as pointed out above. However, the accuracy of any technique, such as an optical sensor, should be thoroughly tested over its entire range of measurement. Surfaces with varying optical constants can cause errors in optical topography measurements. In addition, topography measurements with microscopes are limited to moderate slopes consistent with the range of acceptance angles for the numerical aperture of the objective. Sharp edges, inclusions, defects, and other peculiarities of the surface can scatter light away from the objective and can cause outliers and dropouts of data points in the topographic images measured with optical microscopes, more so than with stylus techniques. Non-linearity in the measured *Z*-position is also a possible source of error for optical-sensing techniques.

In this article, we compare measurements of surface roughness obtained with several techniques over a range of roughness from about 13 to about 500 nm. The techniques include stylus profiling, PSI microscopy, WLI microscopy, and confocal microscopy. Although most of the results are consistent with the expected limitations of these techniques, we observe some surprising differences for WLI with respect to the others.

2 Samples measured

We used interferometrically calibrated step heights to calibrate the *Z*-scale of the instruments or to check the *Z*-scale calibration. For the roughness measurements, we used the roughness average parameters, *Ra* and *Sa* [16, 17], for comparison of the measured topographic results. For a digitized profile, *Ra* is defined as

$$Ra = (1/N)\sum_{i=1}^{N} |Z_i|,$$

where Z_i are the heights of a series of N profile data points measured with respect to the mean line. Analogously, for a surface topography image, *Sa* is defined as

$$Sa = (1/NM)\sum_{i=1}^{N}\sum_{j=1}^{M} |Z_{ij}|,$$

where Z_{ij} is the array of N xM points in a topographic image.

We tested standard periodic gratings with roughness average (*Ra*) ranging from about 60 to 500 nm and random roughness standards with *Ra* values ranging from the sub-nanometer level (i.e., a smooth reference mirror) to about 130 nm. Except for the smooth mirror, the surfaces are highly uniaxial (i.e., the machining marks are oriented along one direction). Therefore, *Sa* results calculated from the topographic images should be very close to *Ra* results calculated from the profiles. The correspondence between *Ra* and *Sa* values would not be as clear-cut for isotropic surfaces or surfaces with complex lay patterns. The surfaces are also highly uniform, so that the variation in the roughness value over each surface is small. These standards are listed in Table 1.

The mirror has a smooth isotropic surface with an *Sa* value approximately equal to the resolution limit of PSI. The mirror is especially useful for estimating the resolution limit for the other optical techniques. The four random samples (Rubert 501–504) [18] are electroformed Ni replicas of steel surface roughness samples fabricated by Song [19, 20] using a hand-lapping process. In addition to being highly uniaxial, the "random" roughness pattern is repeated over distances equal to the recommended profile evaluation length so that the roughness value is highly uniform when measured in widely separated places.

The four periodic surfaces came from three different sources. Two of these (Rubert 528–529) are electroformed Ni replicas of sinusoidal profile roughness samples machined by numerical controlled diamond turning. NIST Standard Reference Material (SRM) 2071 [21] has an electroless Ni surface, diamond turned to produce a sinusoidal profile. The sinusoidal holographic grating has a Au coating providing the surface with a uniform reflectivity.

Table 1 Samples used for the roughness measurements and their *Ra* values with expanded (k=2) uncertainties as measured using stylus instruments

	Sample identification	*Ra* (stylus) (nm)
Random profile samples	Smooth mirror	<0.16 *Sa* (measured with PSI)
	*Rubert 501 [18–20]	14.0±1.8
	Rubert 502 "	34.5±3.4
	Rubert 503 "	88.4±5.8
	Rubert 504 "	129.7±8.6
Sinusoidal gratings	Au-coated holographic grating	58.9±6.8 (period-D≈6.6 μm)
	Rubert 529	103±10 (D≈10 μm)
	NIST SRM 2071 [21]	321.7±8.7 (D≈100 μm)
	Rubert 528	506±29 (D≈50 μm)

*Note: Certain commercial materials are identified in this paper to adequately specify an experimental procedure. Such identification does not imply recommendation or endorsement by NIST, nor does it imply that the materials are necessarily the best available for the purpose

3 Surface profiling techniques

3.1 Stylus

The stylus instrument serves as a standard technique for these comparisons. Therefore, except for the smooth mirror, all surfaces were measured with a stylus instrument, and the *Sa* results obtained with the three types of optical microscopes were compared with the *Ra* results obtained with the stylus. Stylus profiling of the smooth mirror might scratch the mirror and damage its primary function, so PSI serves as the reference technique for the mirror because its noise resolution limit is smaller than that of WLI or confocal.

The stylus profiling measurements were made at several different positions on the surfaces to assess the stability of the roughness values as a function of position. Results for roughness average *Ra* were calculated from the surface profiles and are shown in Table 1. The expanded (k=2) uncertainties of these *Ra* values are comprised of several components, a type-A statistical variation [22] and type-B components due to *Z*-scale calibration, *Z*-scale resolution, uncertainty in the long and short-wavelength cutoffs, and uncertainty in the stylus radius. The *Sa* value obtained by PSI for the smooth mirror is 0.15 nm, small enough that we cannot distinguish the true roughness of the surface from the wavefront deviations and noise of the instrument. Therefore we quote an upper limit for the *Sa* value in Table 1. Because the surfaces are fabricated to function as roughness samples, they have very low waviness and flatness deviations. Therefore, *Ra* values calculated from unfiltered profiles are not significantly different from the values shown in Table 1.

Several stylus instruments were used. For the random surfaces and the Rubert 529 grating, a standard high-pass Gaussian filter [17] with a long-wavelength cutoff of 0.25 mm was used to minimize long spatial wavelengths and a low-pass Gaussian filter with a short-wavelength cutoff of 2.5 μm was used for smoothing. For the Rubert 528 grating, the long-wavelength cutoff was 0.8 mm and the short-wavelength cutoff was 2.5 μm.

SRM 2071 was calibrated in 1989 with a different stylus instrument having a 2RC [17] filter with a long-wavelength cutoff of 0.8 mm. Because the sinusoidal profile has a spatial wavelength of 101.6 μm, the *Ra* value that would be obtained with a standard Gaussian filter with 0.25-mm cutoff is estimated to be within 1% of the value shown in Table 1. SRM 2071 is used periodically as a roughness

check standard in our laboratory and has been shown to have a stable roughness value. The nominal stylus radius was 2 μm for both instruments.

The holographic grating has been tested with several instruments under different conditions. The nominal stylus radius was 2 μm or smaller. The *Ra* value of 58.9 nm shown in Table 1 was measured with a long-wavelength cutoff of 0.25 mm. Measurements taken without a cutoff yield results consistent with that value.

3.2 Phase-shifting interferometric microscope

We performed PSI microscopy using a commercial instrument with a Mirau-type configuration [11]. For all surfaces except SRM 2071, a 50× objective was used having a numerical aperture (NA) of approximately 0.55. The rectangular field of view on the surface was approximately 120×90 μm. For SRM 2071, a 20× objective was used with a field of view of approximately 300×230 μm. The instrument calibration was checked with a calibrated step standard having a 90.65-nm height. For PSI and for the other microscopes as well, *Sa* values were calculated from the topographic images without digital long-wavelength filtering, partly because the topographic images had small fields of view. The field of view along the roughness direction determines the evaluation length and essentially provides the long-wavelength cutoff limit.

For all surfaces except the 503 and 504, average values were calculated from *Sa* results measured in at least three positions. The 503 and 504 standards are difficult to measure with PSI microscopy because of their relatively high roughness and short spatial wavelengths. Measurements from only two positions were used for the 504 and only one was used for the 503. Other measurement attempts on these surfaces produced obvious phase-unwrapping errors [12], which were observed in the topographic images as *Z*-discontinuities producing patches with different apparent heights.

3.3 White light interferometric microscope

We used three different WLI microscopes. One of them (instrument A) was the same instrument as that used for PSI microscopy except that the WLI mode was used instead. The second instrument (B) was a slightly different model instrument from the same manufacturer, and the third (C) was a WLI from a different manufacturer. All were used in the Mirau configuration.

For instruments A and B, a 50× objective was used to measure all surfaces except SRM 2071 for which a 20× objective was used. The fields of view of the topographic images were the same as for PSI. All nine samples were measured with instrument A and seven of them, Rubert 501–504, 528, and 529 and SRM 2071 were measured with instrument B. The *Z*-sampling interval was 80 nm for instruments A and B.

For instrument C, a 50× objective was used with a 2× relay lens. The field of view of the topographic images was approximately 140×110 μm. Four samples were measured, Rubert 502, 504, 528, and 529. For the Rubert 502, the smoothest of these surfaces, three positions were measured. For the other three samples (504, 528, and 529), two positions were measured.

3.4 Confocal microscope

The confocal microscope was the Nipkow-disk type [15]. A 50× objective was used and the field of view was approximately 320×320 μm. The *Z*-scale calibration was checked with a 10-μm step height standard and the *Z*-sampling interval was 70 nm. Topographic images were measured on the smooth mirror, the Rubert 501–504 random profile samples, and all four sinusoidal samples. Three positions were measured for each sample.

4 Roughness measurement results

Figures 2, 3, and 4 show the differences in measured roughness average (*Sa*−*Ra*) values between the optical techniques and the stylus technique. Figure 2 shows generally good agreement between the PSI results and the stylus results for the range of smooth surfaces where PSI is expected to be accurate. These surfaces include the random roughness surfaces with *Ra* ranging up to 130 nm, and the sinusoidal surfaces with *Ra* ranging up to 500 nm. The result for the smooth mirror was not plotted because the stylus was not used to measure it as previously discussed. The *Sa*−*Ra* differences are less than or equal to 6 nm, except for the Rubert 504 and 503 samples with nominal *Ra* of 130 and 88 nm, which have surface slopes that may be high enough

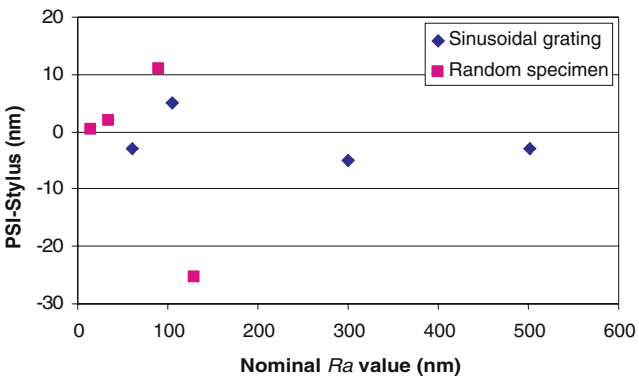

Fig. 2 Differences between *Sa* values measured with the PSI microscope and *Ra* values measured with the stylus technique as a function of the nominal *Ra* value for four random roughness specimens and four sinusoidal profile gratings

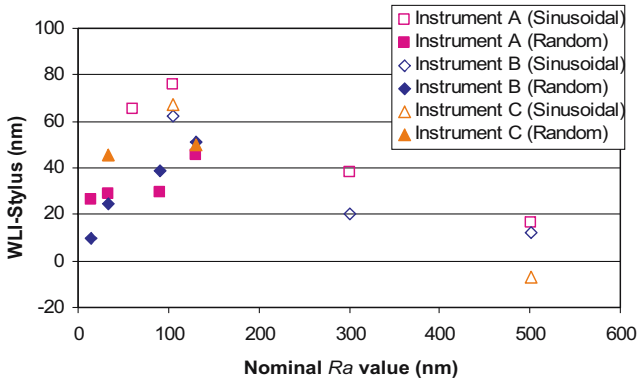

Fig. 3 Differences between *Sa* values obtained with WLI microscopy and *Ra* values obtained with the stylus technique as a function of the nominal *Ra* value. Results are shown for three WLI microscopes and for four random roughness samples and four sinusoidal profile gratings. All eight samples were measured with instrument A, seven with instrument B, and four with instrument C

to cause inaccuracy in the measured roughness topography by PSI because of phase-wrapping issues [12]. High slopes lead to large height differences between pixels, which in turn can cause phase-wrapping ambiguities and hence height measurement errors in the surface profiles. As stated before, only one topographic image was included in the results for the 503 sample because phase-unwrapping errors were observed in the other images. For the rest of the data, the variation in the measured data with position was such that typical standard deviations of the mean were 2.7 nm.

Figure 3 shows larger discrepancies between WLI and the stylus technique than Fig. 2 shows for the PSI. The discrepancies exist for both random and periodic surfaces and seem to peak in the *Ra* range between about 100 and 200 nm. The largest of the observed discrepancies is about 75% of the 103-nm *Ra* value for the 529 standard as obtained with the stylus technique. Typical standard deviations of the mean of the measured *Sa* values are about 6 nm here.

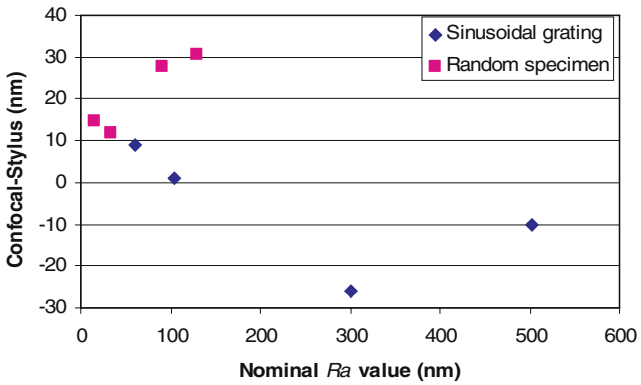

Fig. 4 Differences between *Sa* values obtained with a Nipkow-disk confocal microscopy and *Ra* values obtained with a stylus profiling instrument as a function of the nominal *Ra* value. Results are shown for four random roughness samples and four sinusoidal profile gratings

Results for the three different instruments are shown in Fig. 3, two different models from the same manufacturer and a third instrument from a second manufacturer. The relation between the discrepancy and the *Ra* value, therefore, is not related to a specific WLI instrument. In addition, the shape or the randomness of the sample profile is not an important factor because the differences are observed for both random and periodic surfaces. The differences do not seem to be present if the surface is sufficiently rough or smooth, but seem to be caused by issues in the instrument optics when the surfaces are in a middle range of roughness such that they have a somewhat glossy appearance. Note that for the smooth mirror, the *Sa* value obtained with WLI is 3 nm, which is consistent with the PSI result of 0.16 nm, given the vertical resolution limit of WLI.

The cause of the differences between WLI and the PSI and stylus methods is not yet known to us. We are convinced that the differences illustrated in Fig. 3 are due to the WLI, because the PSI readings in Fig. 2 seem to have no special relation to the *Ra* value.

Figure 4 shows results for a confocal microscope of the Nipkow-disk type. The vertical resolution of this technique is approximately 2 nm, the *Sa* value obtained when the smooth mirror is measured with the confocal microscope. This is in reasonable agreement with the value of 0.16 nm measured with PSI. With respect to the stylus *Ra* results, the confocal *Sa* results seem to be high by about 10 to 20 nm for the random roughness standards and low for the larger amplitude sinusoidal surfaces. Typical standard deviations of the mean are 2.7 nm here.

An important issue is any sensitivity of the *Ra* results to the field of view of the microscopes. For the periodic samples, this is not expected to be significant and only very small differences were obtained when the objective was changed from 50 to 20×. For the random surfaces, both PSI and WLI measurements with the 50× objective yielded topographic images with fewer data dropouts and outliers (invalid points) than with the 20× objective and this is because the 50× objective has a higher numerical aperture and can measure local areas with higher surface slopes than the 20× objective. Also, because the point spacing is closer, phase-unwrapping errors are expected to be smaller for the 50× objective. When we switched from the 50 to the 20× objective on the random samples, in most cases, the measured roughness got slightly smaller.

For the confocal measurements of the random samples, switching from a 50× objective with a field of view of 320 μm to a 20× objective with a field of view of 800 μm yielded increases in *Ra* less than or equal to 5 nm.

Figure 5 shows a portion of four profiles measured for the Rubert 529 standard (100 nm nominal *Ra*) with each of the four profiling techniques. Although the surface is clearly periodic, the sinusoidal profile at this fine roughness level is

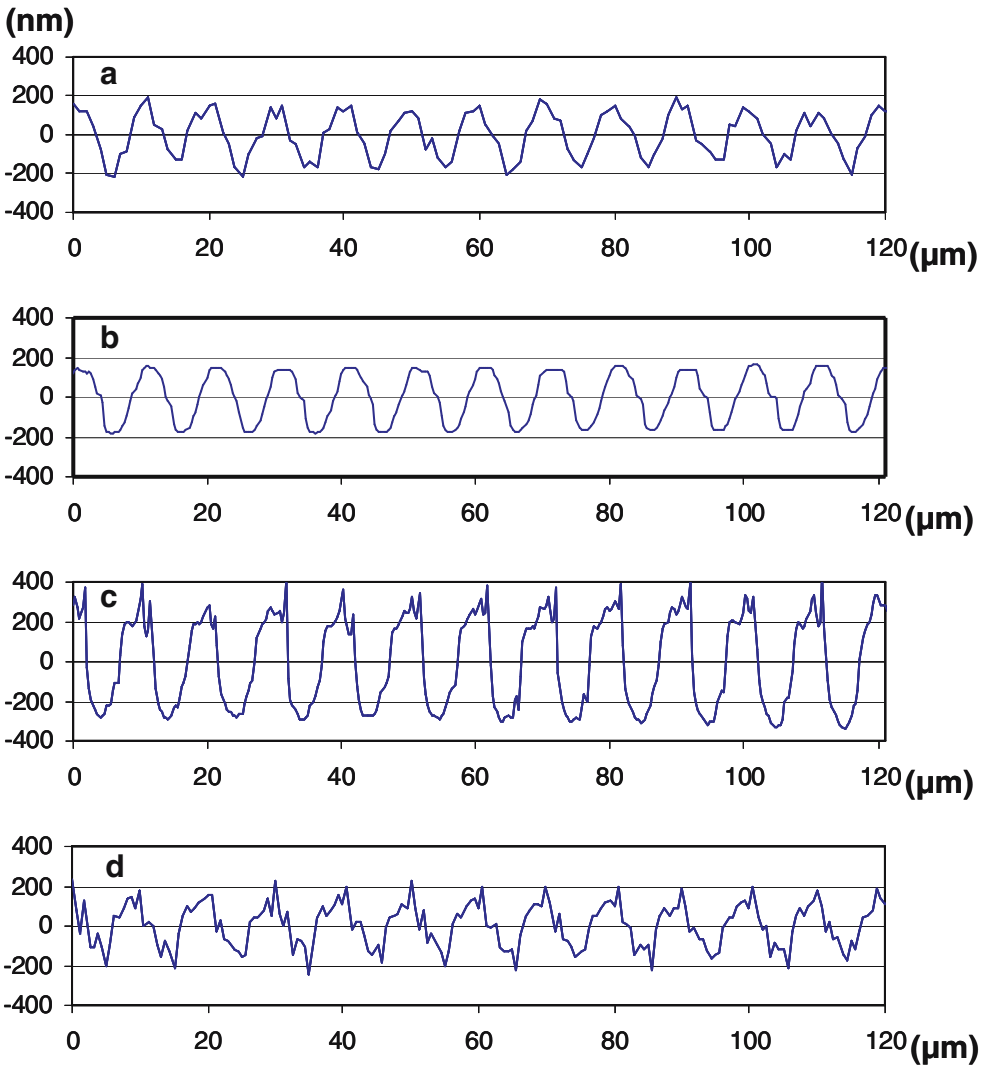

Fig. 5 Profiles of the 100-nm *Ra* sinusoidal grating obtained with four techniques. **a** Stylus. **b** PSI. **c** WLI. **d** Confocal microscopy

imperfect. Despite this distortion of the surface profile, we can observe clear differences between the profiles measured for this surface by the four techniques. The stylus and PSI profiles have about the same amplitude, but the spatial frequency content of the stylus profile seems to be higher whereas the PSI profile seems to be smoother. The WLI profile has higher amplitude, is clearly distorted, and shows noise-like spikes on the grating peaks. Surprisingly, the profile obtained with the Nipkow-disk confocal microscope also shows significant distortion with respect to the stylus and PSI profiles, even though the *Sa* value for this grating obtained with the Nipkow-disk technique is in good agreement with the *Ra* value obtained with the stylus technique.

The confocal microscope exhibits another kind of distortion as well at the 100-nm level of roughness. Figure 6 shows a longer section of the confocal-measured profile than that shown in Fig. 5 and reveals inhomogeneities in the measured amplitude of the surface profile of the holographic grating. The *Ra* measured on the left side of this profile would be larger than the *Ra* measured near the right side of this profile.

Anomalies in the data are significantly smaller at the 500-nm level of *Ra*. Figure 7 shows profiles measured with the four techniques for the Rubert 528 sinusoidal grating,

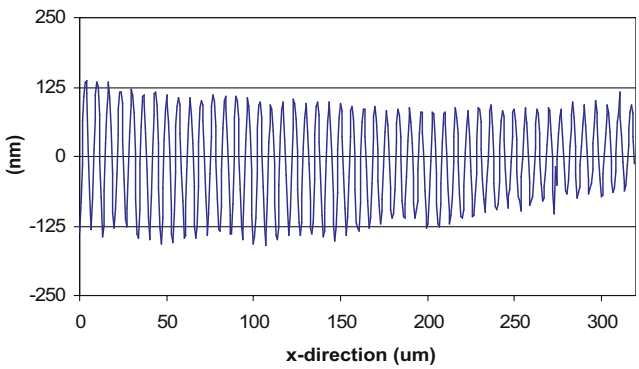

Fig. 6 Profile of Au-coated holographic grating sample 3 obtained with confocal microscopy

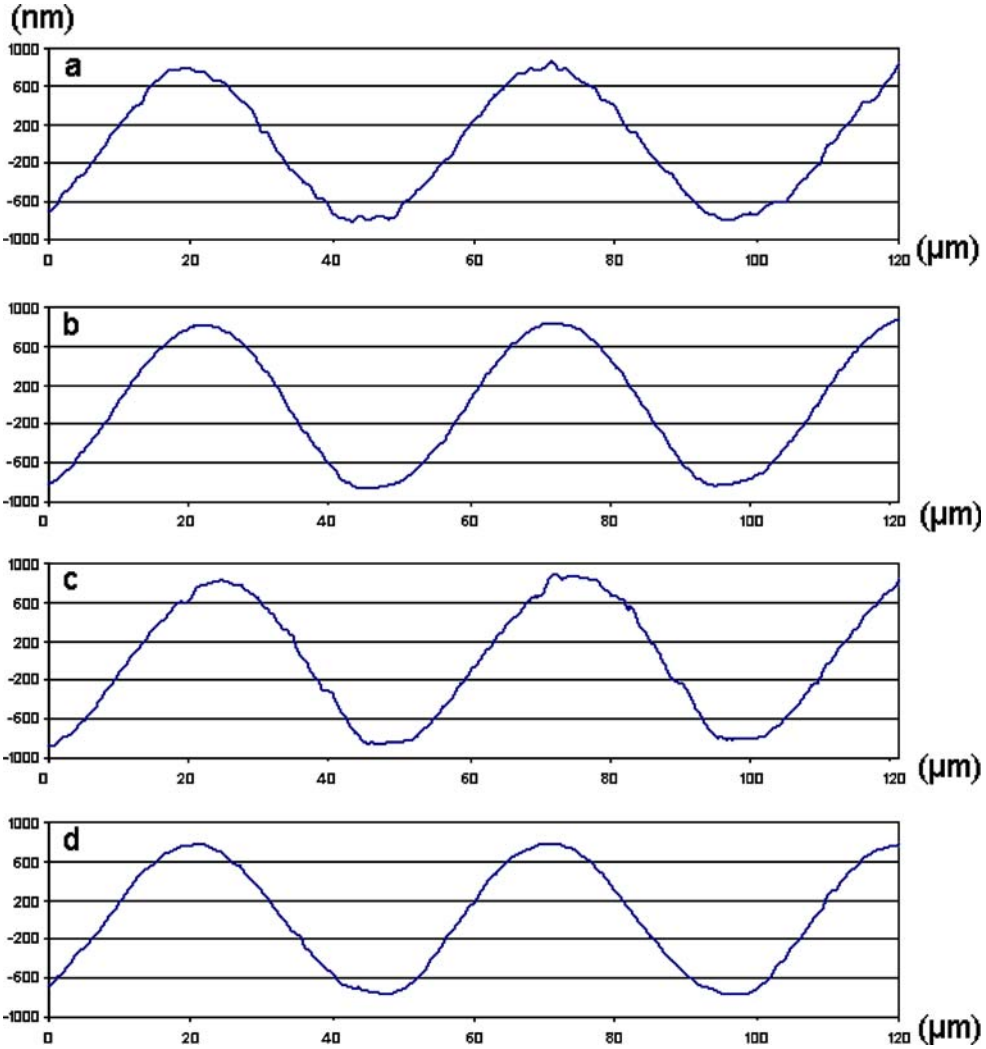

Fig. 7 Profiles of the 500-nm Ra sinusoidal grating obtained with four techniques. **a** Stylus. **b** PSI. **c** WLI. **d** Confocal microscopy

which has 500-nm *Ra* and 50-μm spatial wavelength. The discrepancies between the profiles are now significantly smaller relative to the scale of the surface profile structure than they were for the Rubert 529 grating.

5 Discussion

We have tested periodic grating standards and random roughness standards whose *Ra* values range from sub-nanometer levels to 500 nm. Within this range, the discrepancy between WLI and the stylus instrument shows a special correlation with the surface roughness parameter *Ra*. This discrepancy is especially prominent for *Ra* values between 100 and 200 nm, a transition range of roughness between smooth, specular surfaces and rough, diffuse surfaces. The discrepancy seems to be unrelated to the specific instrument, specimen shape, and randomness. The discrepancy is also unrelated to the spatial resolution of these instruments. The 529 grating, for example, has a moderately long spatial wavelength of 10 μm, which should be easily measurable by microscopes with sub-μm spatial resolution and by styli with 2-μm radii.

In Fig. 3, we have plotted the differences between *Sa* values measured with WLI and *Ra* values measured with a stylus instrument as a function of the *Ra* values. However, it is not yet clear which surface parameters correlate most closely with the measured deviations. Roughness amplitude is clearly important, and the *Ra* value is a good metric of average amplitude for both random and periodic surfaces. Other averaging roughness-amplitude parameters, such as the root mean square (rms) roughness (*Rq*), are also useful measures. However, there does not seem to be a correlation with root mean square (rms) slope of the surface. One indication of this is that the 100-nm and 500-nm sinusoidal surfaces have nominally the same slope but exhibit markedly different profile distortion with respect to the stylus profile. Perhaps surface curvature or peak curvature is the combination of amplitude and wavelength properties that most directly affects the deviations shown in Fig. 5.

The distortions in the measured profiles and the deviations in *Ra* values for WLI may be related to a similar effect observed for step height measurements. WLI has been shown to be susceptible to a skewing effect for step-height measurements when the profile amplitude is less than the coherence length of the light source [23, 24]. The skewing effect leads to spikes in the profile data near step edges. Accurate results for step heights may be obtained by avoiding the edge regions in step-height analysis [23]. Analogously for roughness, regions of high curvature at surface peaks and valleys are similar to sharp step edges and may produce similar profile distortions, as seen for the WLI curve in Fig. 5. A diffraction model is considered elsewhere [25] to describe the phenomenon but does not predict the size of the effect.

Acknowledgements The authors would like to thank N.G. Orji for insightful discussions, D. Cohen for suggestions concerning the direction of this research, and C. Ying for use of one of the instruments. We are also grateful to J. Raja and R.K. Vegesna for assistance with the use of one of the instruments and to S. Phillips and M. Stoudt for their careful reading of the manuscript.

References

1. Vorburger TV, Dagata JA, Wilkening G, Iizuka K (1998) In: Czanderna et al (ed) Beam effects, surface topography, and depth profiling in surface analysis. Plenum, New York, pp 275–354
2. Vorburger TV, Orji NG, Sung LP, Rodriguez T (2003) Surface finish and sub-surface metrology. V-SEMETRA-Fifth Aerospace Metrology Seminar, São Jose dos Campos, Brazil, July 21–24
3. International Organization for Standardization Committee Draft 25178-6 (2007) Geometrical product specification (GPS)-Surface texture: areal - Part 6: classification of methods for measuring surface texture
4. Bennett JM, Tehrani MM, Jahanmir J, Podlesny JC, Balter TL (1995) Topographic measurements of supersmooth dielectric films made with a mechanical profiler and a scanning force microscope. Appl Opt 34:209–212
5. Song JF, Vorburger TV (1991) Stylus profiling at high resolution and low force. Appl Opt 30:42–50
6. Binnig G, Quate CF, Gerber CH (1986) Atomic force microscope. Phys Rev Lett 56:930–933
7. Villarrubia JS (1997) Algorithms for scanned probe microscope image simulation, surface reconstruction, and tip estimation. J Res Natl Inst Stds Technol 102:425–454
8. Lonardo PM, Lucca DA, DeChiffre L (2002) Emerging trends in surface metrology. Ann CIRP 51(2):701–723
9. Rugar D, Hansma P (1990) Atomic force microscopy. Phys Today 23–30, October
10. Hocken RJ, Chakraborty N, Brown C (2005) Optical metrology of surfaces. Ann CIRP 54(2):705–719
11. Bhushan B, Wyant JC, Koliopoulis CL (1985) Measurement of surface topography of magnetic tapes by Mirau interferometry. Appl Opt 24:1489–1497
12. Greivenkamp JE, Bruning JH (1992) In: Malacara D (ed) Optical shop testing. Wiley, New York, pp 501–598
13. Deck L, deGroot P (1994) High-speed noncontact profiler based on scanning white-light interferometer. Appl Opt 33:7334–7388
14. Schmit J, Olszak A (2002) High-precision shape measurement by white-light interferometry with real-time scanner correction. Appl Opt 41:5943–5950
15. Schmidt MA, Compton RD (1992) In: ASM handbook, vol 18. Blau PJ (ed) Friction, lubrication, and wear technology. ASM International, pp 357–361
16. ISO 4287 (1997) Geometrical product specifications (GPS)-Surface texture: profile method-terms, definitions and surface texture parameters. International Organization for Standardization, Geneva, Switzerland, 1997
17. ASME B46.1-2002 (2003) Surface texture (surface roughness, waviness, and lay). Am Soc Mech Eng, New York
18. Rubert & Co Ltd http://www.rubert.co.uk/reference.php.htm, accessed 30 April 2005
19. Song JF (1988) In: Stout K, Vorburger TV (eds) Metrology and properties of engineering surfaces, Proceedings of the fourth international conference. Kogan Page, London, pp 29–40
20. Song JF, Vorburger TV, Rubert P (1992) Comparison between precision roughness master specimens and their electroformed replicas. Prec Eng 14:84–90
21. Vorburger TV, Song JF, Giauque CHW, Renegar TB, Whitenton EP, Croarkin MC (1996) Stylus-laser surface calibration system. Prec Eng 19:157–163
22. Guide to the expression of uncertainty in measurement (GUM) (1995) International Organization for Standardization, Geneva, Switzerland
23. Harasaki A, Wyant JC (2000) Fringe modulation skewing effect in white-light vertical scanning interferometry. Appl Opt 39:2101–2106
24. Harasaki A, Schmit J, Wyant JC (2000) Improved vertical-scanning interferometry. Appl Opt 39:2107–2115
25. Rhee HG, Vorburger TV, Lee JW, Fu J (2005) Discrepancies between roughness measurements obtained with phase-shifting interferometry and white-light interferometry. Appl Opt 44:5919–5927